J. Fluid Mech. (1971), *vol.* 47, *part* 2, *pp.* 305–320
Printed in Great Britain

Instabilities of convection rolls in a high Prandtl number fluid

By F. H. BUSSE

Department of Planetary and Space Science,
University of California, Los Angeles

AND J. A. WHITEHEAD

Institute of Geophysics and Planetary Physics,
University of California, Los Angeles

(Received 29 June 1970)

An experiment on the stability of convection rolls with varying wave-number is described in extension of the earlier work by Chen & Whitehead (1968). The results agree with the theoretical predictions by Busse (1967*a*) and show two distinct types of instability in the form of non-oscillatory disturbances. The 'zigzag instability' corresponds to a bending of the original rolls; in the 'cross-roll instability' rolls emerge at right angles to the original rolls. At Rayleigh numbers above 23,000 rolls are unstable for all wave-numbers and are replaced by a three-dimensional form of stationary convection for which the name 'bimodal convection' is proposed.

1. Introduction

Cellular convection in a fluid layer heated from below, which traditionally has been called Bénard convection, can be regarded as a characteristic example for a gradual transition from laminar to turbulent flow. In contrast to the sudden transition from laminar to non-stationary turbulent flow, which is exhibited by plane parallel shear flows, the instability of a layer heated from below is followed by a number of transitions from one type of stationary cellular convection to another. A large body of experimental and theoretical work has been devoted to the investigation of these transitions in the past decades, starting with the first discovery of a secondary transition by Schmidt & Saunders (1938). In the course of these investigations the following picture of convection in a high Prandtl number fluid has evolved. When the temperature difference across the fluid layer is slowly increased, the static state will become unstable when the buoyancy force is sufficiently strong to overcome the stabilizing effects of viscous dissipation and thermal conduction. The point at which the static fluid first becomes unstable to disturbances of infinitesimal amplitude is described by the critical value R_c of Rayleigh number R, which is the non-dimensional expression for the temperature difference across the layer. Owing to deviations from the Boussinesq assumptions in any real fluid, convection

will first emerge in the form of hexagonal cells as the Rayleigh number is raised above its critical value. When the deviations from the Boussinesq assumptions are small, convection in the form of rolls will replace the hexagons at a Rayleigh number slightly above the critical value. When the Rayleigh number in the conceived experiment is increased further and reaches a value somewhat larger than ten times its critical value, the two-dimensional flow in the form of rolls changes into a three-dimensional pattern which in this paper will be called 'bimodal convection'. Only after the Rayleigh number has reached a much higher, not yet well-determined, value will stationary convection be superseded by non-stationary convection.

Because of these properties, convection in a high Prandtl number fluid is an ideal subject to study typical features of secondary flows. One such feature is the dependence on a wave-number which is an implicit parameter for the secondary solutions of the equations of motion. In the case of convection the wave-number is strikingly exhibited by the cellular pattern of the flow. Solutions of the basic equations corresponding to convection in the form of rolls exist for a relatively large range of wave-numbers α depending on the Rayleigh number R, yet the convection rolls are stable only in a small subrange of wave-numbers. This paper will be concerned with the stability region of convection rolls in the R, α plane and with the instabilities which are responsible for the boundaries of the stable domain.

The stability of two-dimensional convection in the form of periodic rolls with respect to disturbances of infinitesimal amplitude has been analyzed in a paper by Busse (1967*a*) to which we shall refer by (I). An experimental study of the stability of convection rolls was first undertaken by Chen & Whitehead (1968), henceforth to be called (II). In the present paper theoretical, as well as experimental, aspects of the problem will be considered in extension of the work described in (I) and (II). The emphasis, however, will be laid on the experimental investigation.

The idea of the experiment by Chen & Whitehead was to generate convection rolls of a prescribed wave-number by establishing well-defined initial conditions. The fluid layer contained between glass plates was covered with a grid and exposed to a strong light source which produced temperature and velocity perturbations with a well-defined wavelength. The artificially produced perturbations eliminated the influence of the random perturbations and gave rise to convection in the form of rolls with the prescribed wave-number when the Rayleigh number was increased beyond its critical value. As soon as the desired Rayleigh number was reached the source was shut off. Thus the final state of the convection layer, after a stationary state had been reached, was influenced by the additional heating only in the form of the initial conditions. The aspect ratio of the fluid layer used by Chen & Whitehead was rather small, with the consequence that on the average 10 convection rolls were established. Hence the side walls of the circular layer exerted a strong influence on the dynamics of the convection rolls and their instabilities. In the present paper an experiment is described in which the technique of Chen & Whitehead is applied to a rectangular fluid layer of much larger aspect ratio. A typical number of convection

cells (containing two counter-rotating rolls) is 50. The results differ from those described in (II) and demonstrate that a rather large aspect ratio is required to approximate the idealized case of an infinitely extended layer.

The paper starts with an exposition of the physical mechanism of instability in §2. Some theoretical results, based on the same computations as the results reported in (I), are presented in §§2 and 3. The latter section is devoted to the discussion of bimodal convection. 'Bimodal convection' has been chosen as the name for the three-dimensional pattern which represents the only stable form of stationary convection for Rayleigh numbers above 22,600. The experimental apparatus and the method of observations are described in §§4 and 5. The experimental results will be discussed in §6 in comparison with the theoretical predictions.

2. Physical mechanisms for the instability of rolls

We shall start the theoretical part of the paper with a brief review of some general results of the theory of convection. The Boussinesq equations for convection in a horizontal fluid layer heated from below in their usual dimensionless form are

$$\left.\begin{aligned} \nabla^2\mathbf{v}+\mathbf{k}\theta-\nabla p &= Pr^{-1}(\mathbf{v}.\nabla\mathbf{v}+\partial\mathbf{v}/\partial t),\\ \nabla^2\theta-R\mathbf{k}.\mathbf{v} &= \mathbf{v}.\nabla\theta+\partial\theta/\partial t,\\ \nabla.\mathbf{v} &= 0, \end{aligned}\right\} \tag{2.1}$$

where $\mathbf{v}$ is the velocity vector and θ is the deviation of the temperature from the static temperature field. $\mathbf{k}$ denotes the unit vector in the vertical z direction of a Cartesian system of co-ordinates. The rigid boundaries of infinite conductivity require

$$\mathbf{v}=0, \quad \theta=0 \quad \text{at} \quad z=\pm\tfrac{1}{2}.$$

For stationary convection of infinitesimal amplitude the right-hand side in (2.1) is replaced by zero. The resulting linear problem has solutions satisfying

$$\left(\frac{\partial^2}{\partial x^2}+\frac{\partial^2}{\partial y^2}\right)(\mathbf{v},\theta)=-\alpha^2(\mathbf{v},\theta)$$

for all values of α. The lowest eigenvalue R_0 of the Rayleigh number R is a function of α which has a minimum at

$$R_c=1708, \quad \alpha_c=3{\cdot}114.$$

The function $R_0(\alpha)$ is shown by the lower curve in figure 1.

Even though not all solutions of the linear problem correspond to possible solutions of the full non-linear problem in the limit of infinitesimal amplitude, there exists an infinite class of possible stationary solutions of (2.1) for every value of the wave-number α if R exceeds $R_0(\alpha)$. It has been shown by Schlüter, Lortz & Busse (1965), for values of R sufficiently close to the critical value, that the only stable solution is the two-dimensional solution corresponding to convection in the form of periodic rolls. It has been shown also that the convection rolls are stable for a finite range of wave-numbers α which correspond to

somewhat less than one-third of the interval of α for which stationary solutions are possible. In order to extend these results of the analytic perturbation theory to the case of larger Rayleigh numbers, a Galerkin method was employed in (I). Stationary periodic two-dimensional solutions of the equation (2.1) in the case of infinite Prandtl number Pr were obtained for Rayleigh numbers up to 30,000. The stability of the stationary solution was analyzed by superimposing three-dimensional disturbances of infinitesimal amplitude with arbitrary spatial dependence. The calculations have shown that convection rolls are unstable outside the pear-shaped region in figure 1 which is bounded by the curves B and C. The two types of instability which are responsible for the stability boundaries B and C will be described in the following.

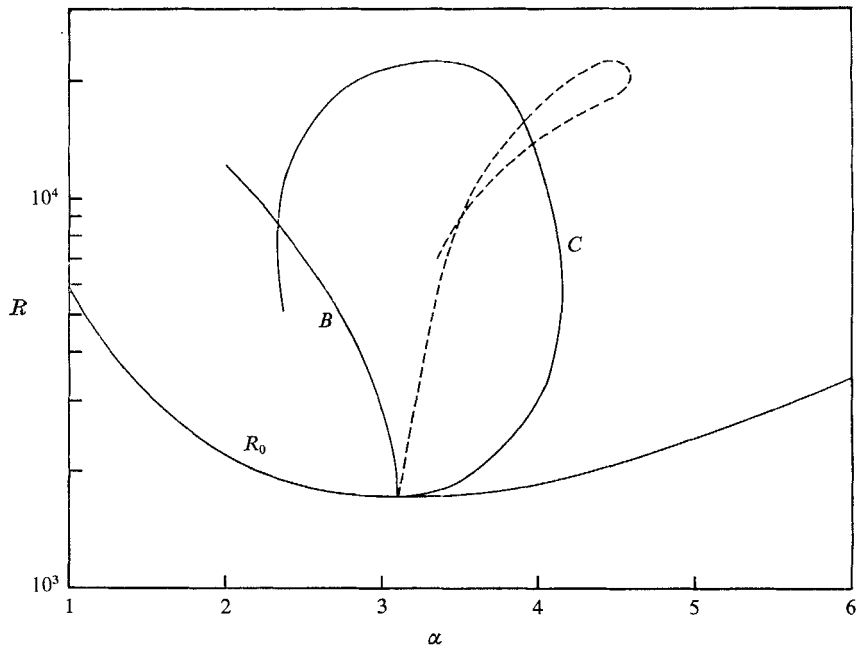

FIGURE 1. Stability region of convection rolls. The zigzag instability and the cross-roll instability produce the stability boundaries B and C, respectively. The dashed line denotes the value of the wave-number $\tilde{\alpha}$ of the marginal cross-roll disturbances along curve C.

The basic reason for the instability of rolls can be understood from the results of the linear theory. There exists a distinguished value α_c of the wave-number at which the convection is optimally adjusted to the geometry of the layer. This property is reflected in the existence of a variational formulation for the linear problem. At small but finite amplitudes an extension of the variational formulation still holds (Busse 1967*b*). The property of optimal adjustment, however, does not distinguish a single value for the wave-number of the physically realized solution at finite amplitudes. Since finite amplitude convection with a given wave-number α modifies the unstable static state of the fluid layer in such a way that the cause for the gravitational instability is reduced, disturbances with a different wave-number will decay in general. Only if the deviation of the wave-number α from the optimal value α_c exceeds a finite threshold value will

disturbances be able to grow and finally replace the original convection pattern by a pattern with better-adjusted wave-numbers. Since periodic rolls represent the only kind of stable stationary convection – at least for sufficiently low Rayleigh numbers – any unstable disturbance will finally lead to a convection pattern in the form of rolls with a wave-number within the stable domain.

Two different instability mechanisms exist at high Prandtl numbers to accomplish the transition from convection rolls with an unstable wave-number to rolls with a stable wave-number. (For a modification of the following discussion at low Prandtl numbers we refer to Busse (1970).) When the wave-number of the convection rolls is too small compared to the optimal value, the effective wave-number can be increased (wavelength decreased) by bending the straight rolls into a wavy roll pattern. We shall call the instability initiating the bending process the 'zigzag' instability. It is responsible for the stability boundary B in figure 1. Mathematically, the instability can be described as a periodic translation of the rolls in the direction perpendicular to their axis which indicates the close relationship to the property of translatorial invariance of the convection solution in the horizontally infinite layer. For rolls with a wave-number higher than the optimal value the zigzag mechanism can only lead to less optimally adjusted rolls and therefore does not occur.

Stationary convection rolls exert a stabilizing influence by the modified mean temperature profile, as well as by the action of the fluctuating temperature and velocity field on any disturbance. Among all possible disturbances of a given wave-number, that which is least affected by the latter influence is most likely to initiate the instability. The theoretical analysis confirms this expectation and shows that disturbances in the form of rolls perpendicular to the given rolls are most effective in changing convection with an excessively large wave-number to a pattern with a more favourable wave-number. This instability mechanism, which we shall call the 'cross-roll' instability, is possible, of course, at large as well as at sufficiently small wave-numbers, in contrast to the zigzag mechanism. It is responsible for the stability boundary labelled C in figure 1.

The foregoing discussion has to be modified for Rayleigh numbers larger than about 15,000. At Rayleigh numbers of this order, convection in the form of two-dimensional rolls does not represent the only form of stable stationary convection.

3. Bimodal convection

The dashed line in figure 1 describes the wave-number of the cross-roll instability in the direction parallel to the axis of the stationary convection rolls at the stability boundary C. The dashed line for $\tilde{\alpha}$ has been obtained by a rough interpolation from the values for the wave-number $\tilde{\alpha}$ of the disturbance with maximum growth rate plotted in figure 2. The latter results are derived from the same numerical work which was described in (I). The difference between the values $\tilde{\alpha}$ corresponding to the left and to the right part of the stability boundary C is small and changes sign at about $R = 9 \times 10^3$. The fact that the dashed line in figure 1 intersects the curve C at about $R = 15{,}000$ implies that the cross-roll

instability cannot lead to stationary convection in the form of rolls for Rayleigh number above the point of intersection. Since $\tilde{\alpha}$ lies outside the range of wave-numbers for stable two-dimensional convection, the stationary asymptotic state is necessarily three-dimensional, if a stable solution of this kind exists. Otherwise, secondary instabilities may occur. The theoretical analysis of infinitesimal disturbances cannot make further predictions at this point. Experiments have shown, in fact, that in most cases a stationary three-dimensional convection

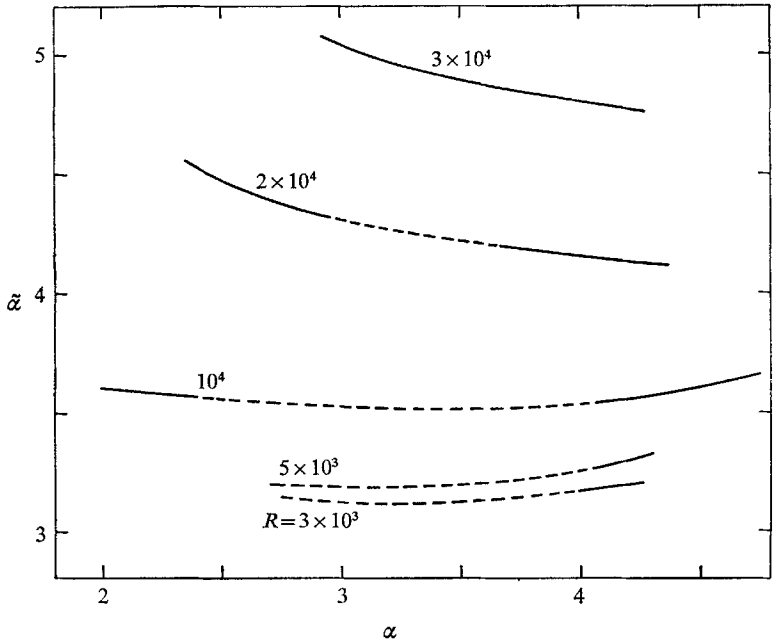

FIGURE 2. The wave-number $\tilde{\alpha}$ of the cross-roll disturbance with maximum growth rate as a function of the wave-number α of the stationary rolls for selected values of the Rayleigh number R. The maximum growth rate is negative in the region of dashed lines.

pattern in the form of bimodal cells is reached as the final state. The term 'bimodal' has been chosen since the three-dimensional convection can be roughly described as the superposition of rolls with a large wave-number on perpendicular rolls with a smaller wave-number and a larger amplitude. The result of the analysis in (I) that two-dimensional convection rolls of any wave-number are unstable for Rayleigh numbers exceeding the value $R_2 \equiv 22{,}600$ emphasizes the fact that the cross-roll instability at high Rayleigh number corresponds to a physical mechanism which is different from the mechanism at low Rayleigh number discussed in the preceding section. Experimental evidence suggests that for Rayleigh numbers in a certain interval beyond R_2 bimodal convection represents the only form of stable stationary convection with the higher wave-number component becoming more prominent as the Rayleigh number increases. Solutions of the basic equations (2.1) describing bimodal convection have not yet been obtained. An understanding of physical reasons for bimodal convection, however, can be gained from the following qualitative arguments.

The two characteristic horizontal scales of bimodal convection suggest a corresponding separation of scales in vertical dimension. A tendency in this direction is indicated by the relative dominance of the higher Fourier components in the z dependence of the growing disturbance leading to bimodal convection. In interpreting this numerical result it was argued in (I) that the gravitational instability of the thermal boundary layer at $z = \pm\frac{1}{2}$ is the principal cause for the cross-roll instability at high Rayleigh numbers. The heat transport carried by convection rolls is not high enough to prevent this instability by keeping the thermal boundary layer sufficiently thin. Bimodal convection demonstrates that two modes adjusted to the boundary-layer scale and the scale of the interior region are more effective at high Rayleigh numbers in carrying the heat across

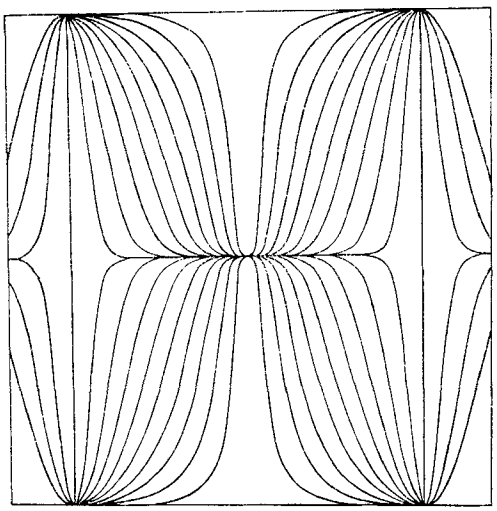

FIGURE 3. Streamlines of bimodal convection. The streamlines for the vector field $(\partial_z v_x, \partial_z v_y)$ at $z = \frac{1}{2}$ have been obtained by multiplying the solution for the marginal cross-roll disturbance at $R_2 = 22{,}600$ with a suitably chosen factor and adding it to the solution of stationary rolls.

the layer than a single mode. The same phenomenon has been found in the theory of the upper bound for the heat transport by convection (Busse 1969). That the transition at the Rayleigh number R_2 is connected with an increase in the heat transport has been observed by Malkus (1954) who used the change in slope of the measured dependence of the heat transport on the Rayleigh number as experimental evidence for transitions. Willis & Deardorff (1967) have recently confirmed the transitions found by Malkus. We refer also to the visual observations by Krishnamurti (1970*a*, *b*). An explanation for the phenomenon that the transition often takes place at a Rayleigh number below R_2 will be attempted in §6.

Since the component with the small wave-number constitutes the dominant part in bimodal convection, the transformation of rolls into bimodal convection by the cross-roll instability represents in general a rather small modification. Thus a fairly accurate picture of bimodal convection can be obtained by adding

to the two-dimensional stationary solution the critical disturbance of the linear stability theory multiplied by a suitably chosen amplitude. In this way the approximate solution for bimodal convection shown in figure 3 has been obtained. The two-dimensional solution and the disturbance of zero growth rate at $R = R_2$ and $\alpha = 3{\cdot}4$ have been used. The figure shows the streamlines of the velocity field close to the boundary of the layer. The picture can be compared with the observation of bimodal convection through a glass plate on top of the layer as shown by figure 8 (plate 1).

4. The experimental apparatus

The control of the initial conditions for the convective instability and the convenient observation of the established convection pattern have been the primary objectives in designing the experimental apparatus. The possibility for accurate measurements of the quantitative properties of convection has been regarded as of secondary importance.

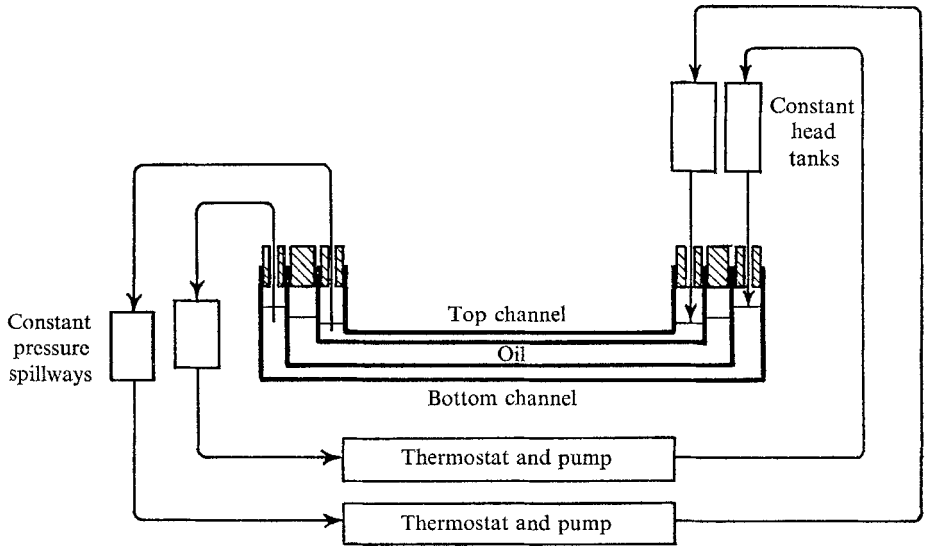

FIGURE 4. Schematic diagram of the experimental apparatus. Arrows indicate water flow, heavy black lines indicate glass, hashed regions indicate styrofoam insulation.

In principle, the apparatus is similar to the one described in (II). As shown in figure 4, the fluid layer containing silicone oil is bounded from below by an arrangement of two parallel glass plates separated by a gap of 0·5 cm. The gap forms a channel through which thermally regulated water is flowing. The same arrangement is used on top of the convection layer. The pattern of convection was observed by shining a slightly diverging beam of light through the fluid layer from below, as shown in figure 5. Owing to the convective temperature field, a ray of light which passes through the layer is deflected through a small angle. The descending cold region of a convection cell, for instance, acts as a convex

lens and produces a bright line as an image of the light source on a screen placed at the approximate focal distance. The photographs on figures 10 to 15 (plates 2–7) show pictures produced in this way.

Controlled initial conditions with a prescribed wave-number were generated by placing a grid on top of the cooling channel above the convection layer. The grid intercepted the light produced by two 500-watt light bulbs at the distance

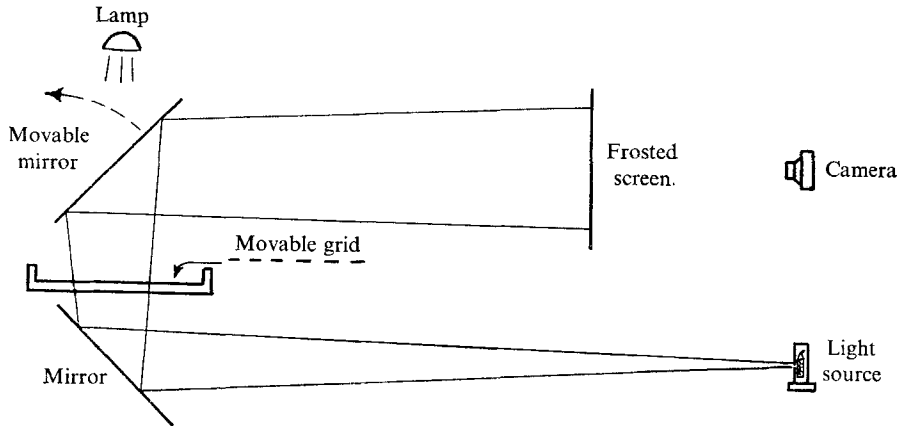

FIGURE 5. Diagram of the observational technique showing movable upper mirror and grid used for inducing rolls.

of 1·5 metres above the convection layer. Thus a temperature perturbation corresponding to the pattern of the grid was produced in the silicone oil. Although the amplitude of the temperature perturbation was less than 0·05 °K, it provided the convection rolls of the corresponding wavelength with a sufficient lead over other random perturbations in the layer. Silicone oil with a low viscosity temperature coefficient was chosen in order to minimize the inhomogeneities of the material properties in the convection layer. The properties of the Dow Corning 200 Silicone oil used in the experiment are

$$\nu = 0{\cdot}10 \text{ cm}^2/\text{sec}, \quad \kappa = 0{\cdot}0010 \text{ cm}^2/\text{sec}, \quad \gamma = 1{\cdot}08 \times 10^{-3}(^\circ\text{K})^{-1}.$$

Because of the low temperature dependence of those properties, the appearance of hexagonal convection could be restricted to a small region just above the critical Rayleigh number. Hexagonal convection is also favoured by a concave or convex temperature profile of the static state at the point of instability. By keeping the mean temperature profile antisymmetric with respect to the mid-plane of the layer, this effect can be avoided. For this purpose the mean temperature of the layer was held nearly constant, while the temperatures in the water channels were changed in an antisymmetric manner.

Special attention was given to the need for uniform horizontal temperatures, careful levelling of the apparatus, and precise dimensions of the convection layer. A uniform horizontal temperature was obtained by providing a sufficiently high flow rate in the water channels above and below the convection layer. The temperature difference between inlet and outlet was kept below 0·2 °K, reaching

this limit only in rather extreme cases. The $\frac{1}{4}$-inch thick glass plates bounding the convection layer can hardly be considered as infinitely conducting, as is assumed in most theories of convection, including (I). Yet the heat conductivity of glass is about six times higher than the conductivity of the silicone oil used in the convection layer. For this reason the finite conductivity of the boundaries should be responsible for only small quantitative deviations from the idealized case considered in the theory. The two temperature baths feeding the water channels were regulated by thermostats which kept the temperature constant within a few hundredths of a degree Kelvin.

The glass plate bounding the lower water channel from below had the horizontal dimensions of 100 cm × 91 cm and a thickness of $\frac{1}{2}$ inch to provide sufficient strength for the apparatus. The horizontal dimensions of the top water channel were 80 cm × 80 cm, leaving space for a reservoir of silicone oil around the convection layer and for the regions of in-and-out flow on opposite sides of the water channels. The plate glass of $\frac{1}{4}$-inch thickness separating the convection layer from the water channels did not have sufficient strength to remain flat unless the hydrostatic pressures of the silicone oil and the water in the two channels was carefully regulated to an accuracy of 1 mm head. The water flow, therefore, had to be constant within 5%, which was achieved by constant head reservoirs for the inlets and by spillways with adjustable height at the outlet of the channels. The resulting head of water at the inlets and outlets was monitored by pressure gauges and was found to stay within the 1 mm limit.

Experiments were carried out for two different depths of the convection layer. For Rayleigh numbers below 10^4, a depth of 5 mm was used; larger Rayleigh numbers were achieved with a depth of 10 mm. By placing the four spacers near to the four corners of the layer at a distance of about 15 cm from the sides and by using the pressure balance described above, a constant depth within a few tenths of a millimetre was attained. Although this accuracy seems to be sufficient in the case of the 1 cm depth, a spatial inhomogeneity was apparent in the experiment with a 5 mm depth. For this reason most of the data at low Rayleigh numbers were obtained using a different apparatus with the horizontal dimensions of 30 cm × 30 cm. With this size a more homogeneous depth of the convection layer was achieved while keeping the aspect ratio comparable to that of the large apparatus at 1 cm depth. In the small apparatus the glass plate bounding the convection layer from below was replaced by a mirror. Thus the beam of light entering the layer from above traversed it twice and produced a strong image of the convection patterns even at rather low Rayleigh numbers.

5. The experimental procedure

The experiments with a depth of 5 mm and with a depth of 10 mm differed because of the characteristic response time d^2/κ of the convection layer. This effect is partly offset by the fact that changes in the convection pattern occurred faster at higher Rayleigh numbers. For this reason the times used in connexion with the low depth experiment described below were multiplied by a factor between 2 and 4 for the 1 cm depth experiment. At the start of an experiment the convection

layer was left for at least 15 min at a subcritical Rayleigh number to establish a static state of pure conduction. After this time a grid of the desired wavelength was placed on top of the apparatus and the heat lamp was turned on. For this purpose the top mirror shown in figure 5 was pulled back. After about 10 min the thermostats were set to their final values, with the consequence that the temperature difference between upper and lower water channels increased at a rate of 1 °K per minute. A few minutes after the final temperature difference was reached the heating lamp was turned off, the grid removed, and the top mirror set in place. A light beam emerging from a 0·4 cm hole in front of a tungsten filament bulb was shone through the oil layer and projected the convective pattern on to a frosted screen. The observations were recorded by taking photographs at appropriate intervals. When the convection rolls were unstable, the first signs of instability became apparent immediately after the observation started, or some minutes later. In the case of the wavy instability, it took sometimes 15 min before indications of bending of convection rolls were observed. Stable convection rolls remained unchanged for hours. Sometimes a pinching instability travelled from the side wall into the field of view, or a new roll was generated at the side wall, leading to a slight compression of the pattern. The question of stability was usually decided half an hour after the observation had started. However, the observations continued until the convection pattern was changed to a new quasi-stationary pattern. Since the instabilities did not occur homogeneously throughout the new layer, convection cells established by the instability were usually correlated only over a region of a few wavelengths in diameter. Accordingly, the new quasi-stationary pattern showed a patchy structure similar to the convection produced by a change from subcritical to supercritical Rayleigh number with random initial conditions.

The Rayleigh number was not measured directly in the experiments. Using the calculations for the heat transport by convection rolls in (I), the Rayleigh number was computed from the temperature difference between the water channels, taking into account the finite conductivity of the glass plates. The influence of the temperature boundary layer in the water channel itself can be considered as small and was neglected for this reason. Because of their indirect deduction, the values for the Rayleigh number can be incorrect by several per cent. An accurate determination of the Rayleigh number was not regarded as important because most parts of the stability boundary in the R, α plane depend only weakly on the co-ordinate R.

6. Discussion

The principal result of the experiment is shown in figure 6. The comparison of the observed instabilities with the calculated stability boundary indicates qualitative agreement between experiment and theory. The finite conductivity of the glass plates bounding the convection layer appears to be responsible for the shift of the experimental values relative to the theoretical curve. A rough theoretical estimate shows that the heat conductivity of the glass, which is six times the conductivity of the silicone oil, is responsible for a 5 % decrease of the

critical wave-number α. This result is in approximate agreement with the observations. The fact that the effective conductivity of the fluid layer increases with the Rayleigh number owing to the convective transport, can be used as an explanation for the increasing shift between the data and the theoretical curve. The analogous discrepancy is apparent in figure 7 in which the observed wave-number $\tilde{\alpha}$ of the cross-roll instability has been plotted as a function of the

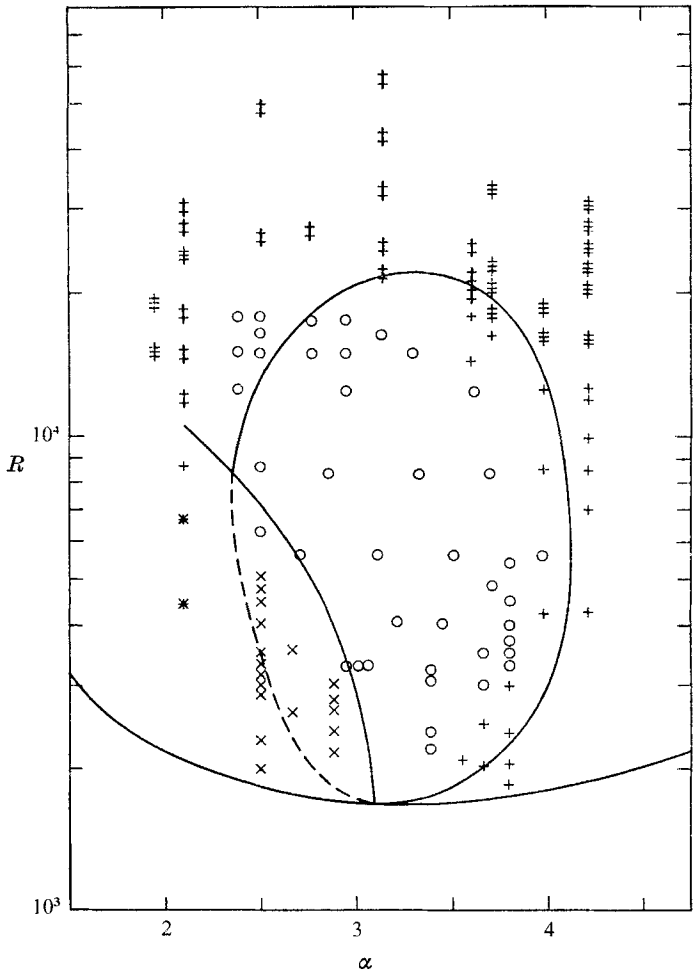

FIGURE 6. Experimental results. ○, stable rolls; ×, zigzag instability; +, cross-roll instability leading to rolls; ∓, cross-roll instability leading to bimodal convection; ∓, cross-roll instability inducing transient rolls with subsequent local processes. The curves correspond to the theoretical results shown in figure 1.

Rayleigh number. The value of $\tilde{\alpha}$ does not depend on the wavelength of the basic rolls. The latter has been indicated only roughly in the figure by using the letters L, M, S for large, medium, and small-sized rolls, respectively. For $R \geqslant 10^4$, within a relatively large scatter, a slight tendency can be noticed for rolls with low wave-number (large rolls labelled L) to become unstable to cross-rolls of

greater wave-number $\tilde{\alpha}$ than rolls with a high wave-number (small rolls labelled *S*). This is in agreement with theoretical results shown in figure 2.

The change in the convection pattern induced by the cross-roll and the zigzag instabilities is exhibited in figures 10 to 14 (plates 2–6). The zigzag instability was observed for Rayleigh numbers up to about 8000. It occurred sometimes

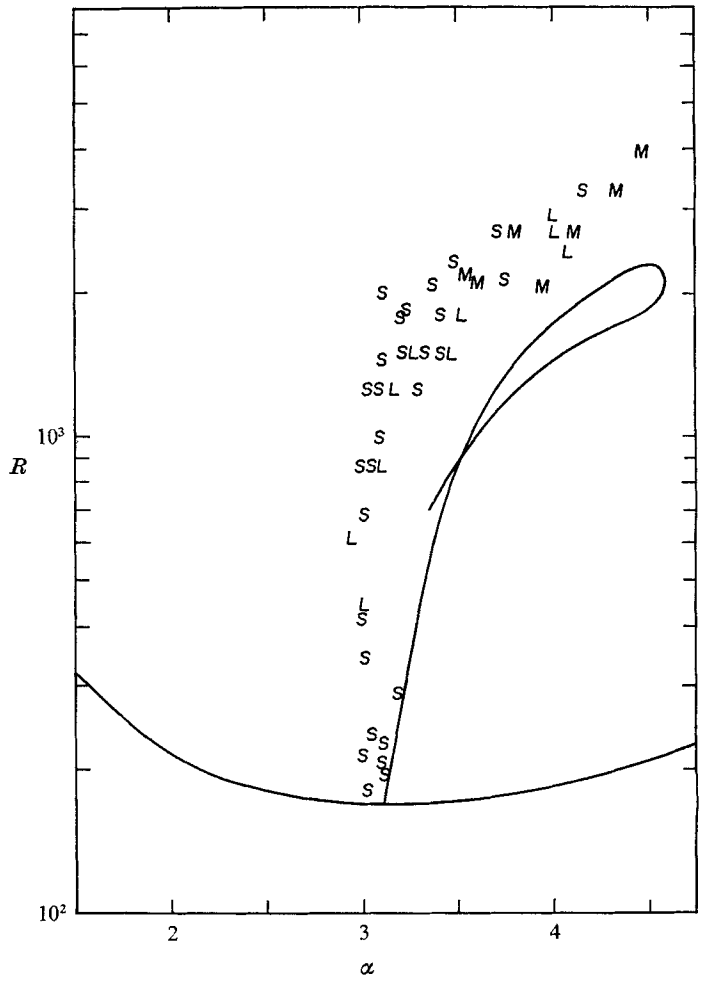

FIGURE 7. The observed wave-number $\tilde{\alpha}$ of the cross-roll instability as a function of the Rayleigh number R. The letters L, M, S indicate that the instability occurred on rolls with large, medium, or small wavelength. The solid line represents the theoretical result from figure 1.

simultaneously with the cross-roll instability in agreement with the comparable growth rates given by the stability theory. Since the wavelength of the zigzag instability was always a little smaller than the wavelength of the original rolls, the zigzagging continued to become accentuated until an angle of nearly 45° was reached. At this point the 'zigs' of a roll cell and the 'zags' of the neighbouring cell joined to form a new roll cell, as shown in figure 11. Since rolls of opposite inclination to the original rolls are produced with equal probability, the

final pattern showed a rather patchy structure. The cross-roll instability does not have this additional degree of freedom; thus the convection pattern produced by this instability showed large regions of uniform rolls perpendicular to the original pattern.

In (II) the observation of the zigzag instability was mentioned only briefly since the cross-roll mechanism appeared to be the dominant instability for small wave-number as well as for large wave-numbers. This difference between the results of (II) and the present experiment indicates the strong influence of the lateral boundaries.

At large Rayleigh numbers the onset of the cross-roll instability resembled the onset at low Rayleigh numbers. As the cross-roll disturbances evolved, however, they were succeeded by complex local processes when the Rayleigh number exceeded a value of about 15,000 and the wave-number of initial rolls was either above 3·8 or below 2·1. Owing to their high wave-number, the cross-roll disturbances could not generate stable rolls or bimodal cells. Although rolls with a corresponding wave-number were established as a transient pattern, they were soon transformed by more localized processes into a pattern of larger wavelength as figures 12 and 13 indicate. To a certain extent the local processes can be identified with the pinching mechanism which we shall discuss below.

While the cross-roll instability of rolls with large or with very small wave-numbers is followed by radical changes of the original convection pattern, a gradual transition to bimodal convection takes place for rolls of intermediate wave-number. The transition in the neighbourhood of the Rayleigh number $R_2 = 22{,}600$, in particular, involved such small changes that the stability boundary could not be very well defined by the present observational technique. This, together with the fact that no hysteresis was observed at the reversed transition from bimodal cells to rolls, suggests that the bimodal solution of the stationary Boussinesq equation branches off the two-dimensional solution at an infinitesimal amplitude of the three-dimensional component.

Figure 14 illustrates the transition to bimodal convection while the Rayleigh number is increased slowly beyond 20,000. The shadowgraph pictures of bimodal convection are in agreement with the observations by Rossby (1969) and Krishnamurti (1970*a*) and with the picture shown in figure 8, which was taken from an unpublished experiment by Willis. As the Rayleigh number increases the cross-roll component of the bimodal convection becomes more pronounced, as evidenced by the increased sharpness of the secondary pattern. No transition, however, to a different type of convection was found for Rayleigh numbers up to 70,000. This observation seems to disagree with the findings of Krishnamurti (1970*b*) and the transition at about $R = 5 \times 10^4$ in the heat transport data measured by Malkus (1954) and Willis & Deardorff (1967). However, as Krishnamurti mentions, the transition to non-stationary convection at $R = 5 \times 10^4$ seems to occur as a rather local phenomenon and may be suppressed by the fairly homogeneous pattern in the present experiment.

When the cross-roll instability does not lead directly to a new stable stationary pattern, the situation resembles the case of convection generated from random initial conditions. In addition to the variation of the wave-number, the relative

orientation of the convection cells plays an important role. One of the processes by which the convection field rearranges itself locally is the pinching mechanism. In its idealized form the pinching mechanism combines two roll couplets into a single couplet by joining the ends of two adjacent rolls. To illustrate this mechanism an experiment was performed in which two sets of rolls with parallel axes were generated. The wavelength of the two sets had a ratio of 2:3. Figure 15 shows that the pinching effect extends the larger rolls at the cost of the smaller rolls. The large cell always seems to be favoured over the smaller cells, even if the large cell subsequently becomes unstable to the cross-cell instability. The pinching mechanism seems to be one of the causes for the change towards smaller wave-number, which is usually observed in convection experiments when the Rayleigh number is increased. The tendency towards large-sized rolls is responsible for the fact that the transition to bimodal convection occurs often at Rayleigh numbers much lower than 22,600, as has been shown by Krishnamurti (1970*a*).

One of the fascinating phenomena of convection generated from random initial conditions in a layer of very large aspect ratio is the fact that the pattern continues to change, even though the exterior conditions are kept stationary. The characteristic time scale of the changes, of course, is increasing strongly as time goes on. One may speculate about the large-scale pattern which will be achieved asymptotically at moderate Rayleigh numbers in the absence of any influence from lateral boundaries. In the present study questions concerning this problem have been answered only in part. In addition to the wave-number, the curvature of rolls appears to be a relevant parameter in stability problems. It is to be expected that the asymptotic state will consist of regions of slightly curved rolls. Since changes will continue to occur at the edges between different regions, it remains an interesting question whether a strictly stationary pattern can be achieved starting from arbitrary initial condition.

The authors are indebted to Paul A. Cox for the skilful construction of the apparatus. Figure 8 was kindly supplied by G. E. Willis. The research was supported by N.S.F. Grant GA-10167.

REFERENCES

Busse, F. H. 1967*a* On the stability of two-dimensional convection in a layer heated from below. *J. Math. and Phys.* **46**, 140–149.

Busse, F. H. 1967*b* The stability of finite amplitude cellular convection and its relation to an extremum principle. *J. Fluid Mech.* **30**, 625–649.

Busse, F. H. 1969 On Howard's upper bound for heat transport by turbulent convection. *J. Fluid Mech.* **37**, 457–477.

Busse, F. H. 1970 Stability regions of cellular fluid flow. *Proceedings of the IUTAM-Symposium*, Herrenalb 1969. In press.

Chen, M. M. & Whitehead, J. A. 1968 Evolution of two-dimensional periodic Rayleigh convection cells of arbitrary wave-numbers. *J. Fluid Mech.* **31**, 1–15.

Krishnamurti, R. 1970*a* On the transition to turbulent convection. Part 1. Transition from two to three-dimensional flow. *J. Fluid Mech.* **42**, 295–307.

Krishnamurti, R. 1970*b* On the transition to turbulent convection. Part 2. Transition to time-dependent flow. *J. Fluid Mech.* **42**, 309–320.

MALKUS, W. V. R. 1954 Discrete transitions in turbulent convection. *Proc. Roy. Soc.* A **225**, 185–195.

ROSSBY, H. T. 1969 A study of Bénard convection with and without rotation. *J. Fluid Mech.* **36**, 309–335.

SCHLÜTER, A., LORTZ, D. & BUSSE, F. 1965 On the stability of steady finite amplitude convection. *J. Fluid Mech.* **28**, 223–239.

SCHMIDT, R. T. & SAUNDERS, O. A. 1938 On the motion of a fluid heated from below. *Proc. Roy. Soc.* A **165**, 216–228.

WILLIS, G. E. & DEARDORFF, J. W. 1967 Confirmation and renumbering of the discrete heat flux transition of Malkus. *Phys. Fluids*, **10**, 1861–1866.

FIGURE 8. Photograph of bimodal convection at $R = 25 \times 10^3$ in an experiment by G. E. Willis. The convection layer contains silicone oil with $Pr = 450$ and is covered by a glass plate.

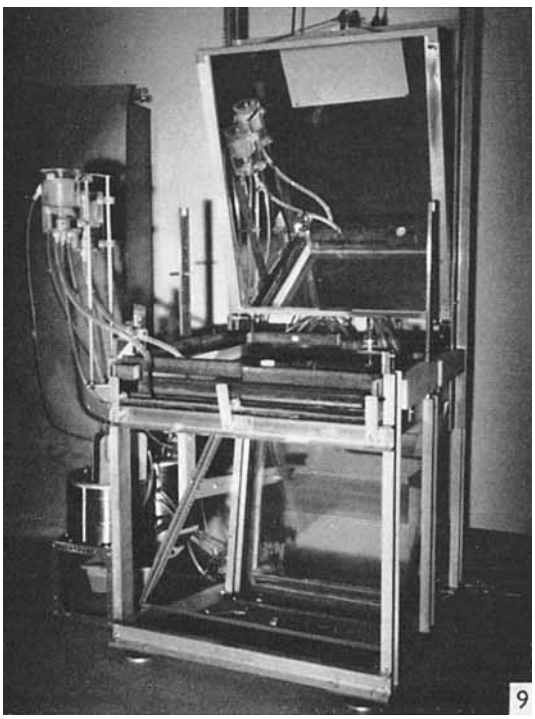

FIGURE 9. Experimental apparatus with lifted top mirror.

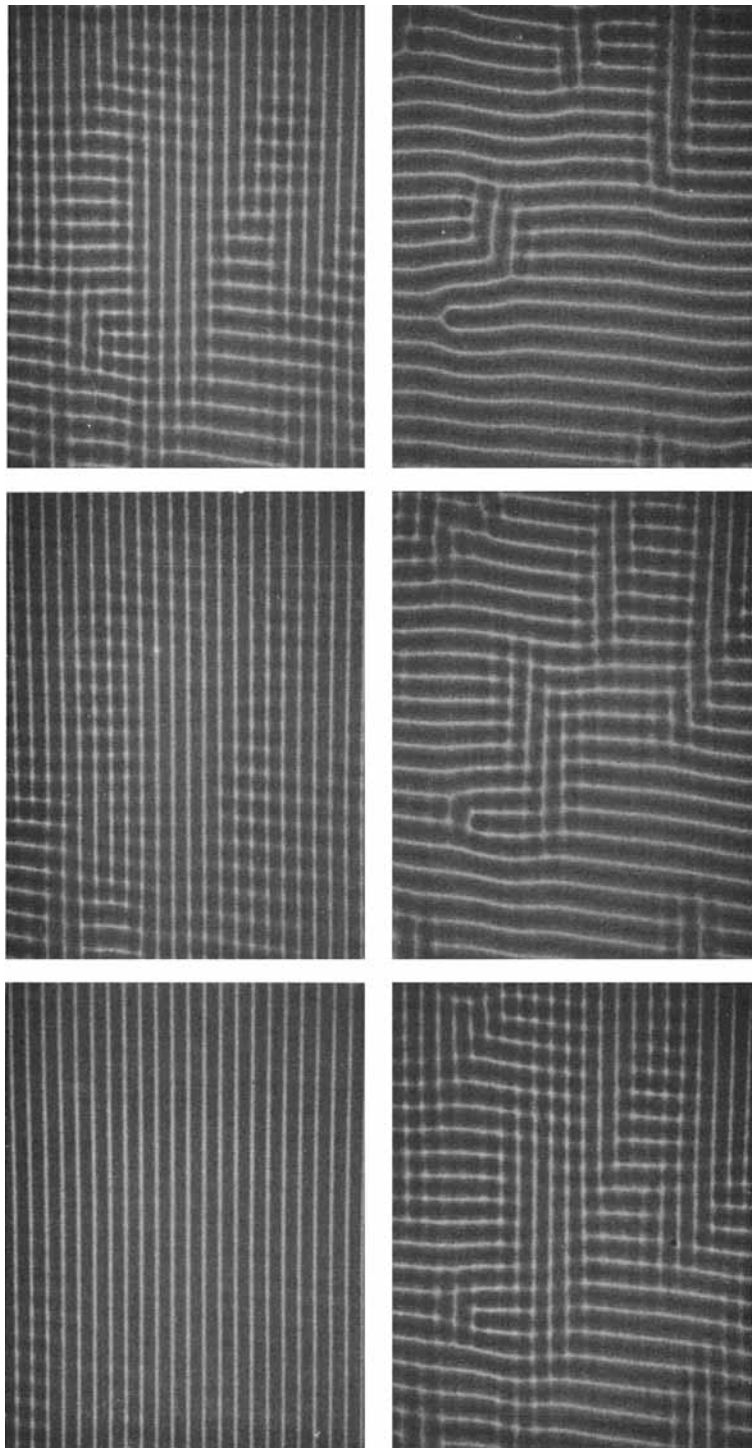

FIGURE 10. Cross-roll instability at $R = 3000$, $d = 5$ mm, $\alpha = 2\pi/1{\cdot}64$. Time intervals between subsequent photographs are 10, 4, 3, 7, and 28 min, respectively.

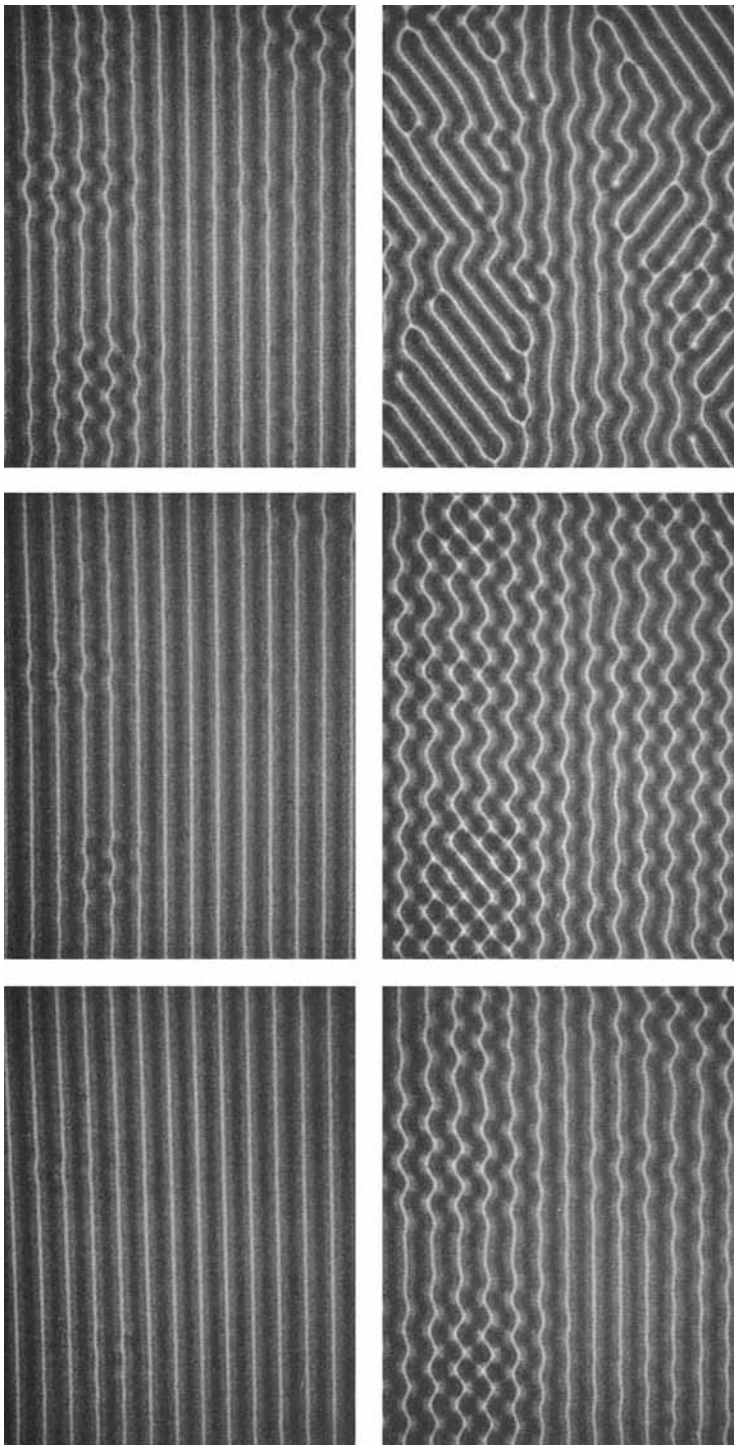

FIGURE 11. Zigzag instability at $R = 3600$, $d = 5$ mm, $\alpha = 2\pi/2{\cdot}8$. Time intervals between subsequent photographs are 9, 10, 10, 26, and 72 min, respectively.

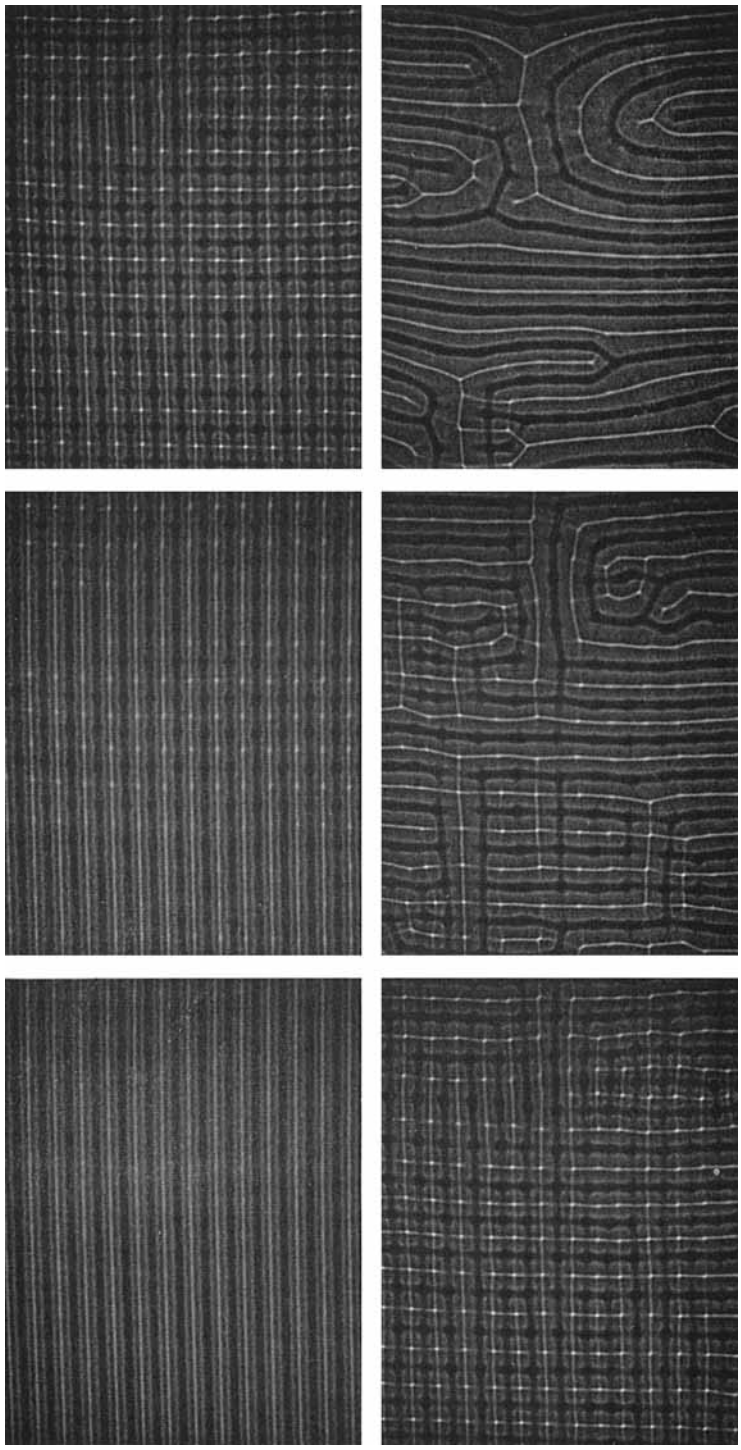

FIGURE 12. Cross-roll instability at $R = 21 \times 10^3$, $d = 1$ cm, $\alpha = 2\pi/1{\cdot}5$. Time intervals between subsequent photographs are 4, 8, 4, 10, and 24 min, respectively.

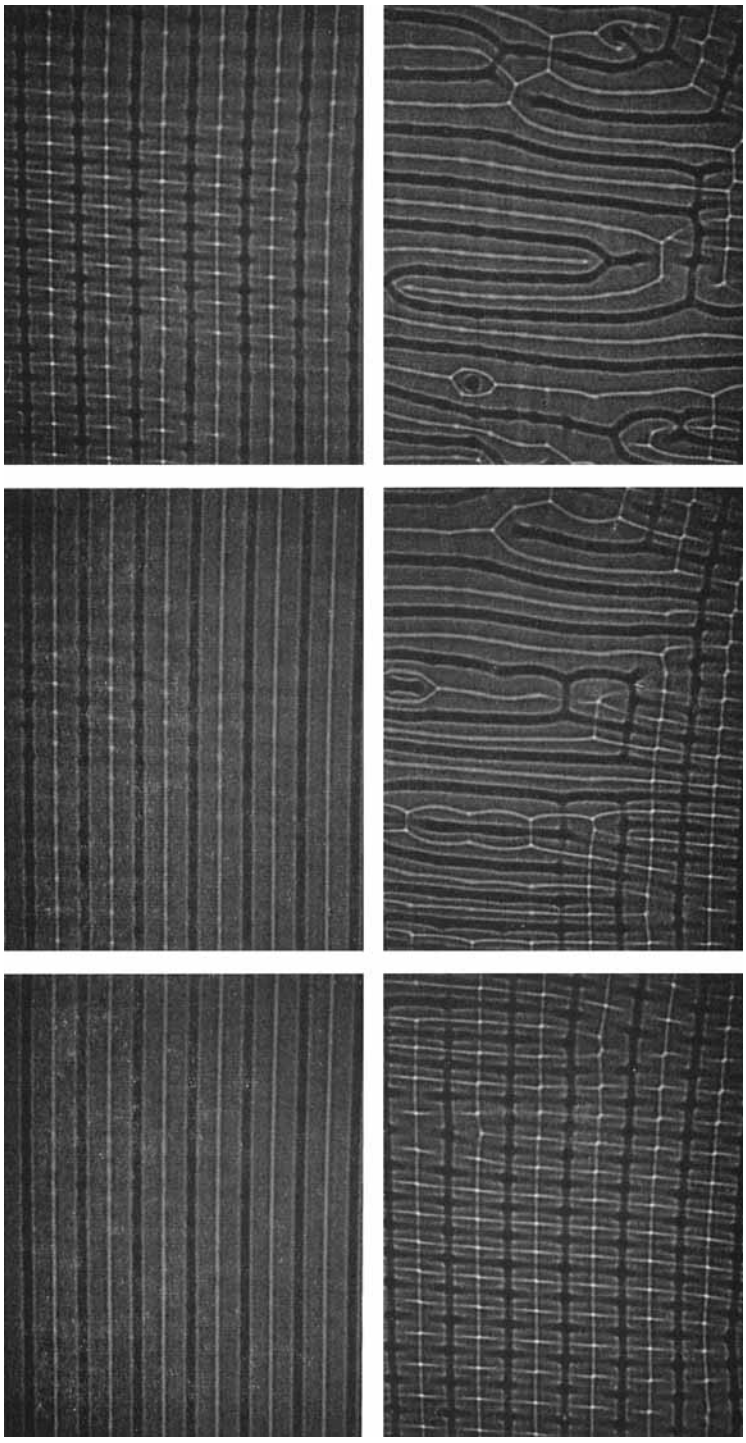

FIGURE 13. Cross-roll instability at $R = 24 \times 10^3$, $d = 1$ cm, $\alpha = \frac{2}{3}\pi$. Time intervals between subsequent photographs are 5, 10, 25, 35, and 25 min, respectively.

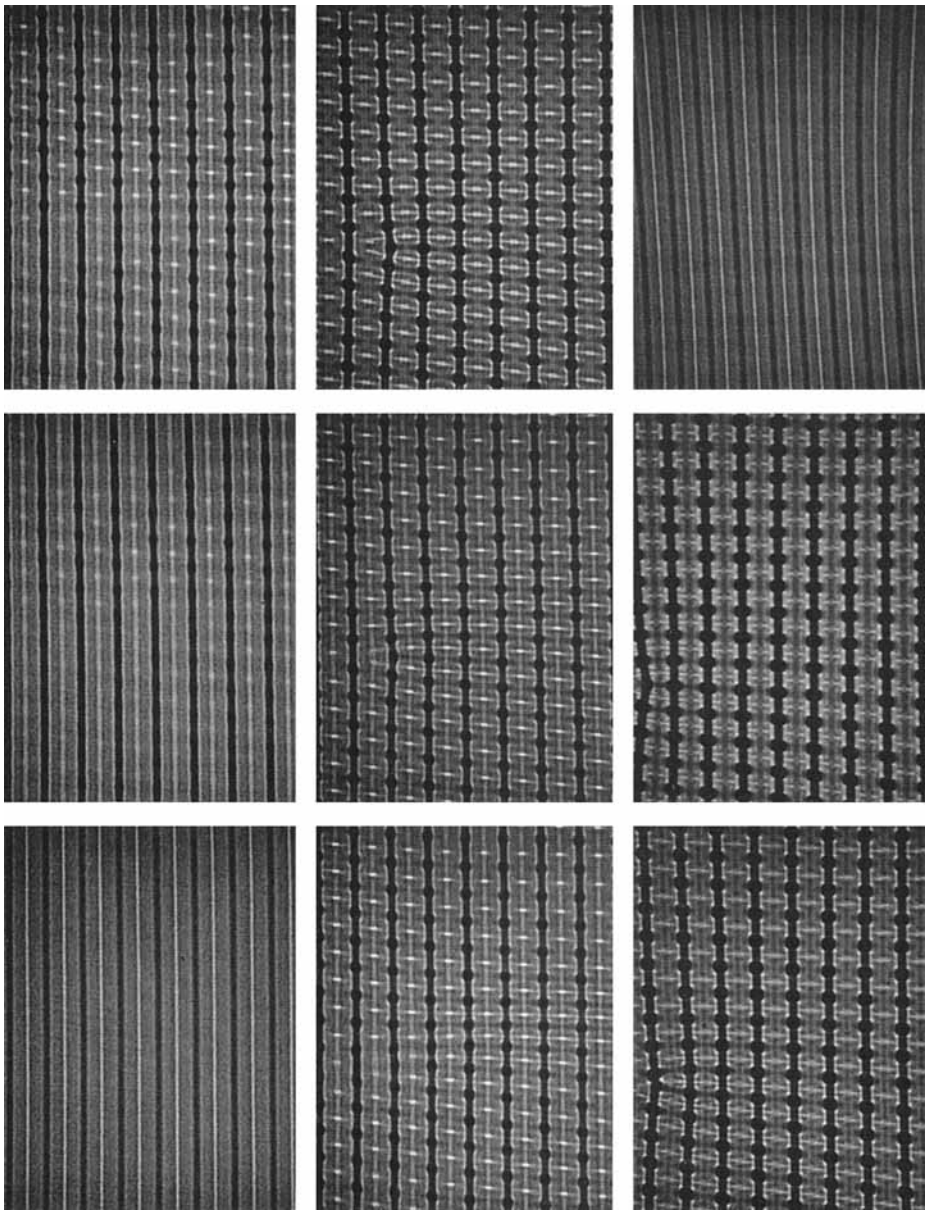

FIGURE 14. Bimodal convection. R increases slowly in time from 20×10^3 to 65×10^3 over a space of 4 hours. The last photograph was taken 10 h after R has been decreased to the original value 20×10^3.

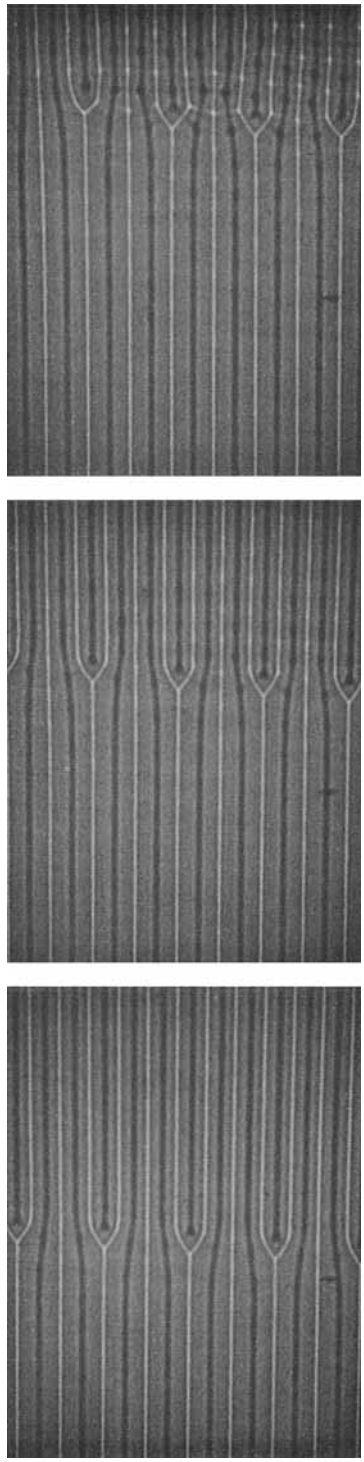

FIGURE 15. Pinching instability at $R = 18 \times 10^3$, $d = 1$ cm, $\alpha_1 = 2\pi/2{\cdot}55$, $\alpha_2 = 2\pi/1{\cdot}7$.
The time interval between the photographs is 35 min.